Carbon Pellet Injection Experiments at the Stellarator W7-AS

L. Ledl, R. Burhenn, V. Sergeev[1], S. Egorov[1], B. Kuteev[1], L. Lengyel, S. Skokov[1], F. Wagner and W7-AS team, ECRH Group[2], NBI Group

Max-Planck-Institut für Plasmaphysik, EURATOM Ass., D-85748 Garching, Germany
[1]St. Petersburg State Technical University, 195251 St. Petersburg, Russia
[2]Institut für Plasmaforschung, Universität Stuttgart, D-70569 Stuttgart, Germany

Introduction - Prediction of the spatial deposition profile of ablated pellet atoms is of fundamental interest for many possible applications of impurity pellet injection such as diagnostic of plasma parameters (using injection of Li, B, C pellets), plasma fuelling (LiD, LiT) and wall conditioning (Li, B) in magnetically confined hot plasmas. It presumes the basic understanding of the main physical processes involved in the dynamic of the ablation process. For simplicity of interpretation, the plasma of the advanced stellarator Wendelstein 7-AS offers the possibility for such investigations under net current-free conditions (internal currents < 10kA) and in the absence of main rational surfaces due to its extremely low magnetic shear. In order to study the nature of the ablation process with better spectroscopic access, carbon pellets were injected into W7-AS plasmas by a gas-dynamic injector. The dedicated pellet diagnostics allow highly resolved temporal and spatial detection of selected spectral carbon line emission along the pellet trajectory from which the ablation rate can be deduced. The analytical NGS (neutral gas shielding) model /1/ was applied for simulation of the experimental radial ablation rate profiles.

Experimental set-up - Carbon pellets of 370-410μm diameter (corresponding to (1.2-1.6) 10^{18} C-atoms) were accelerated by an one-stage pneumatic injector /2/ up to velocities of 200-400 m/s, using 20-40 bar helium as propellant gas. The injector is connected to the vessel of W7-AS (R=2m, a=18cm, B=2.5T) by a slightly curved guiding tube (1.5m length, 2mm diameter, bending radius 3.5m). The injection system provides small amount of propelling gas (< 10^{16} atoms) additionally introduced into the plasma. After leaving the guiding tube the pellets have a stray angle of approximately 3 degree FWHM. As shown in fig.1, the pellet penetration process is spatially imaged from the bottom side by two CCD-cameras (1,2), measuring simultaneously the spectral emission of two different ionization states, and from the rear side by a third CCD-camera (12). The interline-type CCD-cameras (PCO-FlashCam, PCO-SensiCam) are principally capable to accumulate up to 10 snap-shots with high time resolution. For ablation studies, the exposure time was generally increased in order to exceed the whole pellet lifetime. Additionally, a fast semiconductor diode (11) provides time traces of the ablation light. All cameras and the diode are supplied with interference filters (7,8,9,10) for detection of spectral line radiation of selected ionization states of carbon.

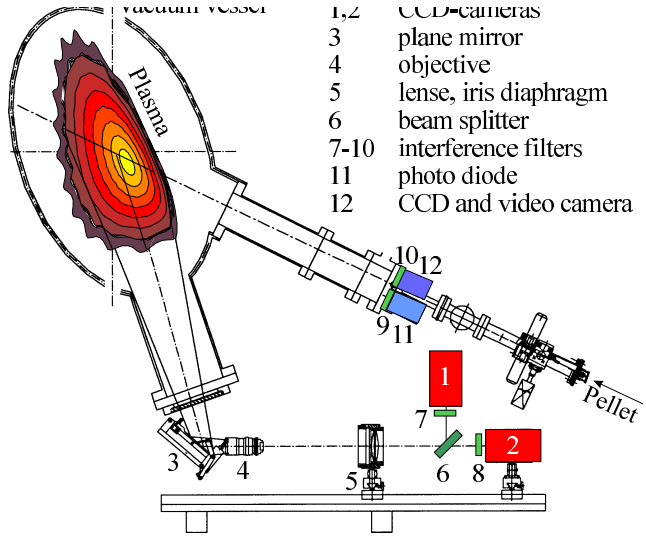

Fig.1 : Injection geometry at W7-AS and experimental instrumentation for pellet observation

General investigations - For ablation rate measurements, some milestones have to be confirmed: the center of gravity of the emitting ablation cloud is identical with the pellet position; the pellet does not disturb plasma temperature in front of the pellet position (no pre-cooling wave); the observed spectral light is proportionally related to the ablation rate; the radial pellet velocity remains unchanged during traversing the plasma. Latter allows us to relate local and temporal spectral line emission measured by CCD-camera and the diode.

The picture of CII pellet cloud light measured using CCD camera (2) is shown in fig.2, where the x-axis represent the effective plasma radius and the y-axis the toroidal direction along the magnetic field lines. We can see from this picture a symmetric distribution of the pellet cloud light in toroidal direction along the radial pellet path in the plasma. The similar result was obtained for the poloidal distribution of the pellet cloud light, measured using snap-shot exposures by CCD-camera observation from the rear side (12). The instant pellet position should be assumed at the maximum of these symmetric toroidal and poloidal light distributions. As a result, no evidence for a toroidal and poloidal drift of the ablation cloud was found. A significant asymmetry of pellet cloud light relative to the instant pellet position along the direction of the pellet trajectory could be excluded by time-integrated CCD-pictures. For this purpose the exposure of the bottom-side CCD cameras (1,2) was shortly interrupted (Δt=30μs) during path-in-flight of the pellet. The drop in intensity along the pellet trajectory at the start of the shutter time interval is symmetric to the increase at the end of the shutter time interval. The steepness of both the drop and rise in this time-integrated picture is determined by the width of pellet cloud light in the direction perpendicular to the magnetic field line as it was measured by snap-shot CCD pictures. Consequently, it can be concluded that no significant radial drift of the C^{+1} ions in the pellet cloud took place during the interruption of the exposure at least on the time scale less than the ionization time of these ions. Accumulated high repetition snap-shot pictures along the pellet trajectory always reveal a throughout constant radial pellet velocity. In net-current free ECF (electron cyclotron frequency)-heated discharges even no toroidal acceleration of the pellet was observed. On the contrary, in ECF-heated discharges with fairly significant net plasma current (>5 kA by electron cyclotron current drive) but also in NBI (neutral beam injection)-heated plasmas, bending of the pellet trajectories in toroidal direction were observed.

The absence of radial acceleration of the pellets offers the possibility to transform the time traces of the carbon radiation, detected by the fast semiconductor diode, into a radial emission profile, showing up fairly good agreement with the time-integrated but spatially resolved CCD camera pictures as shown in fig.3. From fast electron temperature measurements (Δt=1μs) using ECE (electron cyclotron emission) diagnostics, no indication for pre-cooling of the plasma was found along the way towards the plasma core. From fig.2,3 a significant decrease of pellet cloud emission and ablation rate can be seen when the pellet crosses the plasma core.

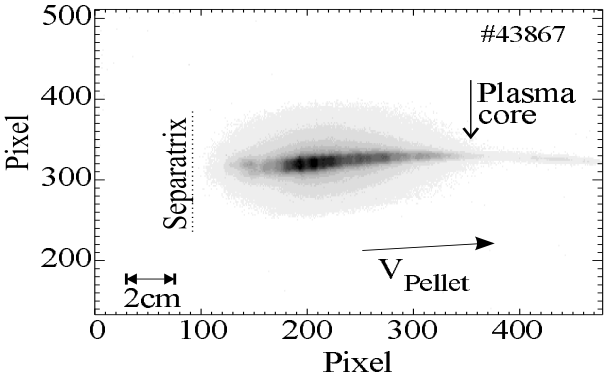

Fig.2: Pellet trajectory as seen from CCD camera 2 behind CII-filter, integrated over the pellet lifetime. Locations of separatrix and plasma center are marked

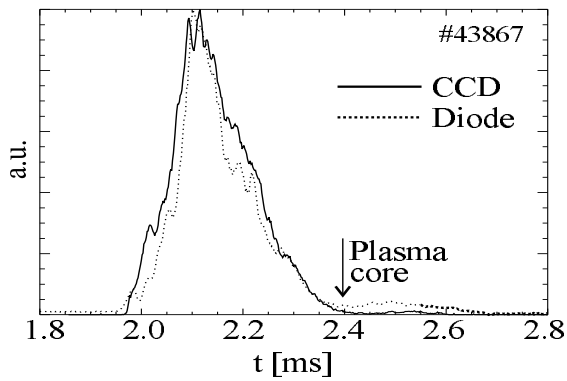

Fig.3: Temporal evolutions of CII emission measured by the diode and CCD camera 2.

Ablation rate measurements - The ablation rate profile was calculated from the observed CII line emission (dominant transition $3p^2P^o$-$3d^2D$, 723.1/723.7nm) assuming a direct proportionality between both. This approach /1/ is based on the consideration that ionization and excitation in the whole pellet cloud are dominated by the „hot" electrons of the ambient plasma. In this case, a proportional relation can be achieved under the assumption of a nearly constant ratio between ionization and excitation rate. If the „cold" electrons ($T_e \approx 1$eV) within the pellet cloud would contribute significantly to or even dominate the atomic processes, as shown in /3,5/, this simple approach cannot be assumed a priori due to the strong dependence of the rate coefficients on electron temperature below 10eV. Additionally, no detailed experimental knowledge about the plasma parameters in the cloud are available yet. In order to proof the

validity of the assumed proportionality experimentally, the local change in electron density profile after pellet injection was calculated using the derived local ablation rate and compared with radially resolved measurements from multichannel interferometer. Because pellet deposition length and plasma size in W7-AS have comparable dimensions, this comparison is not as conclusive as in TFTR /4/, but the deposition profile derived from CII emission could principally be confirmed, even with regard to the limited sensitivity. Additionally, calculations with a quasi-three-dimensional pellet code /5/ show that the proportional relation between C II line emission (723nm) and pellet ablation rate is not drastically varying (0.7-1.0) within the dominant ablation region measured in experiments.

The spectral width covered by the detected CII lines was spectroscopically measured to be approximately 1nm and the maximum shift of the central wavelength of the interference filters due to non-paraxial rays is 0.6nm, which is still within the 10nm transmission window of the filters. The continuum radiation contributes 5% per nanometer to the observed CII line emission (723.1/723.7nm), being 50% for the filters (spectral width 10nm) mainly used in the present experiments. This value of continuum contribution was derived by comparison of the detected radiation using filters with different spectral width (10nm/2nm) but the same central wavelength. The ratio of continuum to line radiation along the pellet trajectory, however, was observed to be nearly constant. Therefore, this does not falsify the proportionality between measured CII radiation and the ablation rate.

NGS-model - During traversing the plasma, the C-pellet will be heated by heat flux parallel to the magnetic field lines. The carbon atoms which are evaporated during the pellet lifetime of approximately 1ms form a cold and dense neutral gas cloud around the pellet. When getting ionized, the cloud expands along the magnetic field lines. The used spherical symmetric steady-state NGS-model /1/ considers the reduction of the heat flow to the pellet by absorption of energy within the neutral ablation cloud around the pellet only. From the remaining heat flow to the pellet, the ablation rate then is deduced. In this model, an adiabatic cloud expansion has been assumed. The analytical expression for the pellet ablation rate was obtained under the assumption of weak shielding when the shielding factor $\delta=Q_e/Q_{eo}$ of the ablation cloud being defined as the ratio of electron heat flux on the pellet surface Q_e to the flux Q_{eo} far from the neutral cloud satisfy the relationship $1-\delta<<1$. Possible usage of this expression for lower δ values of 0.3-0.5 has been proofed by comparison with predictions from the impurity neutral gas shielding code by Parks et al. /4/. In the case for carbon pellets injected into the ECRH-discharges δ values of 0.4-0.8 were deduced. For the pellet-specific material properties, the measured pellet density $\rho=0.9$ g/cm^3 (for pellet size of $d\approx0.4$mm) and the thermo-chemically heat of ablation of 4 eV/atom in the case of cluster ablation mechanism /6/ at pellet surface temperatures of approximately 4500 K, were used as input for the NGS-modelling.

Modelling of experiment and discussion - According to the magnetic field geometry of W7-AS, the magnetic field strength, generated by a system of discrete non-planar coils along the plasma axis, varies periodically around the machine, resulting in a certain magnetic field ripple and the existence of magnetic mirrors. The machine consists of 5 identical torus modules. At the positions where the modules come into touch large ports were installed that lead to a discontinuity in the toroidal coil (module field B_m) equipment. 5 additional large-size non-planar coils (B_s) are located at these positions in order to reduce the introduced magnetic field ripple. By changing the current ratio I_s / I_m of the two coil systems, the magnetic field strength could be varied along the toroidal direction. As a result, at the ECRH launching position ($\phi=36^o$) shown in fig.4 either a magnetic minimum („standard"-configuration) or maximum („B_{max}"-

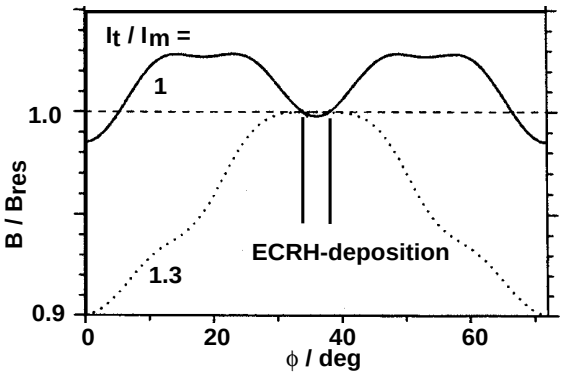

Fig. 4: Example for relative magnetic field strength on axis within one field period for standard configuration (I_t / I_m=1, solid line) and B_{max}-configuration (I_t / I_m = 1.3, dotted line).

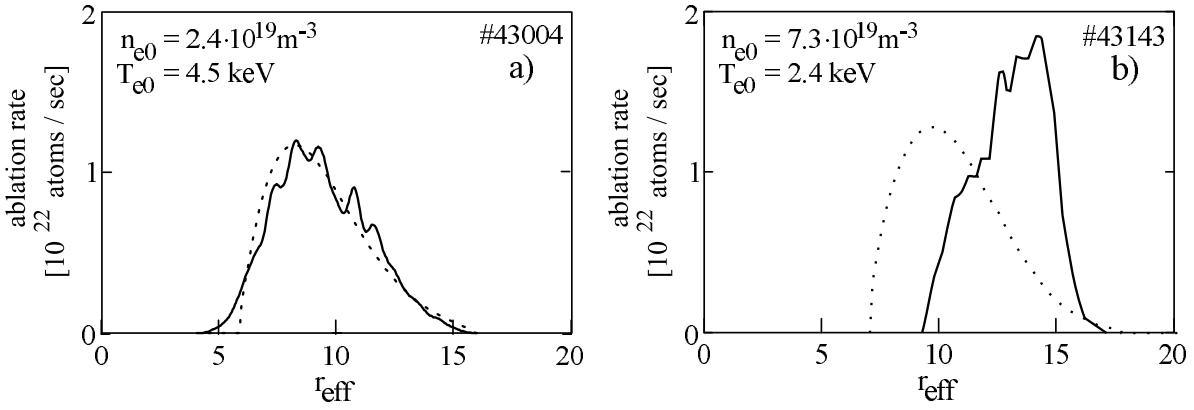

Fig.5: Comparison of ablation rate profiles deduced from the measured CII-line emission (solid lines) and those calculated by the NGS model (dotted lines): a) „B_{max}"-configuration and b) standard-configuration.

configuration) can be generated keeping the resonance condition for ECRH (140GHz, 2.54T). Carbon pellet injection experiments were performed using these two types of magnetic configuration (with ι=0.34, P_{ECRH}=1.2 MW). The existence of a certain stray angle during injection required a full 3-dimensional determination of the pellet trajectory by the observation diagnostics, in order to relate the correct local electron density and temperature to the pellet ablation position.

As shown in fig.5, principally different features in the spatial CII-radiation profile and, consequently, in the ablation behaviour were observed in these two scenarios. For the „B_{max}"-configuration, fairly good agreement could be achieved between the measured ablation rate profile and that predicted by the NGS model. On the contrary, in „standard"-configuration discharges the maximum of the ablation rate profiles is significantly shifted towards larger effective plasma radii and could not be reproduced by the NGS-model which tooks into account a Maxwellian energy distribution of electrons. A possible approach to explain this discrepancy might be the existence of additional electron heat flux on the pellet surface. Because this feature was observed in different magnetic configurations we could speculate about the behaviour of suprathermal electrons in these different magnetic scenarios.

Due to the existence of a magnetic mirror in the „standard"-configuration at $\phi=36^{o}$, trapped suprathermal electrons are expected in front of the ECRH-launching plane. Both passing and trapped electrons within the ECRH-deposition zone in the plasma core region, gain perpendicular energy from the resonant ECF-heating waves. Only the passing electrons are able to thermalize their energy by collisions in the region close to the plasma center. The trapped electrons are expected to be driven towards larger radii due to a grad B-drift mechanism /7/ until they are scattered into the loss cone of the mirror. Therefore, the fraction of trapped electrons in the ECRH-launching plane would lead to an effective broadening of the ECRH-deposition profile and an increased population of suprathermal electrons in outer plasma regions, where the enhanced ablation occurs - even at higher densities (fig.5b). In the „B_{max}"-configuration, a magnetic hill is located in front of the ECRH-launching plane, giving rise to the assumption that the population of suprathermal electrons at larger radii is not so pronounced and their effect on the ablation process should be smaller. The study of the „enhanced" ablation process is subject of ongoing investigations.

References

[1] B.V. Kuteev, V.Yu.Sergeev and L.D.Tsendin, Sov. J. Plasma Phys. **10** (1984) 1133.
[2] P.T. Lang *et al.*, Rev. Sci. Instrum. **65** (1994) 2316.
[3] A.G. ElCashlan *et al.*, Phys. Fluids B **12** (1992) 4166.
[4] V.Yu. Sergeev *et al.*, Rev. Sci. Instrum. **63** (1992) 4984.
[5] A.Ushakov *et al.* This conference.
[6] C.A. Klein *et al.* J. Applied Phys. **65** (1989) 3425.
[7] M. Rome *et al.* Plasma Phys. Control. Fusion **39** (1997) 117.o